New Dielectric Elastomers with Variable Moduli

*Wei Hu, Zhi Ren, Junpeng Li, Erin Askounis, Zhixin Xie, and Qibing Pei**

Dielectric elastomers have been widely investigated for muscle-like soft actuators and capacitive sensors. Mechanical properties play a central role in the performances of the active material. Most elastomers have specific moduli pre-determined by the polymers' molecular structures, which are not suitable for applications in changing working conditions as natural muscles are capable of. Here new dielectric elastomers are described exhibiting variable moduli controlled via thermal treatment. The elastomers contain furan-maleimide Diels–Alder adduct moieties to administer the crosslinking densities of the elastomeric networks via reversible Diels–Alder/retro-Diels–Alder cycloaddition reaction, resulting in changes in the elastomers' moduli. One of the synthesized elastomers has moduli that can be controlled between 0.17 and 0.52 MPa incrementally and reversibly. Capacitive strain sensors based on this elastomer can be operated in both rigid and soft modes to achieve variable sensing response up to 30% linear strain. Actuators were fabricated and operated in both high strain mode (35% actuation area strain at 65 MV m^{-1}) and high force output mode (0.55 MPa at 104 MV m^{-1}). The elastomers can exhibit a range of stress–strain outputs in similar fashion as muscle.

1. Introduction

Dielectric elastomers are a type of electroactive polymers with the general moniker of artificial muscle thanks to their mechanical compliancy, large actuation strain, high energy density, and light weight.[1,2] Dielectric elastomers are being investigated for a slew of electromechanical devices such as soft actuators, large-strain capacitive sensors, and mechanical energy harvesters.[3–5]

The electromechanical responses of dielectric elastomers are greatly influenced by the materials' mechanical properties such as modulus, elongation of rupture which defines the boundary for the maximum performances, and viscoelasticity which affects response speed. The actuation strain of a dielectric elastomer actuator is determined by

$$s_z = -\frac{\varepsilon_0 \varepsilon_r E^2}{Y'} \tag{1}$$

where s_z, ε_0, ε_r, E and Y' are the transverse strain, vacuum permittivity, dielectric constant of the elastomer, applied electric field, and apparent modulus of the elastomer, respectively.[6] Although the actuation strain could be tuned through changing the applied electric field, in some electroactive systems, variable strain is needed while constant actuation pressure ($\varepsilon_0 \varepsilon_r E^2$) is maintained. Therefore, elastomers with tunable moduli would be desirable in these cases such as adaptive grippers and microfluid channels.[7,8] These elastomers can further mimic natural muscles, which is able to adapt to changing working requirements.[9]

Previous strategies to achieve tunable stiffness in polymers include application of magnetic field onto a magnetorheological elastomer,[10] use of ultraviolet light to change the microstructure of a liquid crystal polymer[11] and controlling the phase transition through altering the temperature of shape memory polymers.[12] However all these material systems require maintaining the external stimuli during operation, which would add on the device complexity, energy consumption, and shortens useful lifetime. We propose a new elastomeric material whose stiffness can be altered via simple thermal treatment, and multiple states with different stiffness are all stable at room temperature.

A synthetic elastomer generally has a specific modulus predetermined by the polymer's molecular structure. In the theory of rubber elasticity, the tensile modulus (Y) of an ideal elastomer at small strain is determined by

$$Y = \frac{3\rho RT}{\overline{M_c}} \tag{2}$$

where ρ, R, T, and $\overline{M_c}$ are the density of the elastomer, the gas constant (8.31 J K^{-1} mol^{-1}), the absolute temperature, and the average molecular weight of chain segments between crosslinking sites, respectively.[13] $\overline{M_c}$ is also a term to describe the crosslinking density of an elastomer network, where a larger $\overline{M_c}$ means a lower crosslinking density. As indicated in Equation (2), polymer chain segment length is a key factor of an elastomer's stiffness. Therefore, our strategy tuning the stiffness is to change the chain segment length using dynamic covalent bonding, which could reversibly form and break crosslinking sites as illustrated in **Figure 1**.

Diels–Alder (DA) reaction offers an effective method to form dynamic covalent bonds, and has been widely utilized in self-healing materials thanks to the good reversibility of the DA reaction.[14] Among DA pairs, furan derivatives as the diene and

Dr. W. Hu, Z. Ren, Dr. J. Li, E. Askounis, Z. Xie, Prof. Q. Pei
Department of Materials Science and Engineering
University of California–Los Angeles
420 Westwood Plaza, Los Angeles, CA 90095, USA
E-mail: qpei@seas.ucla.edu

DOI: 10.1002/adfm.201501530

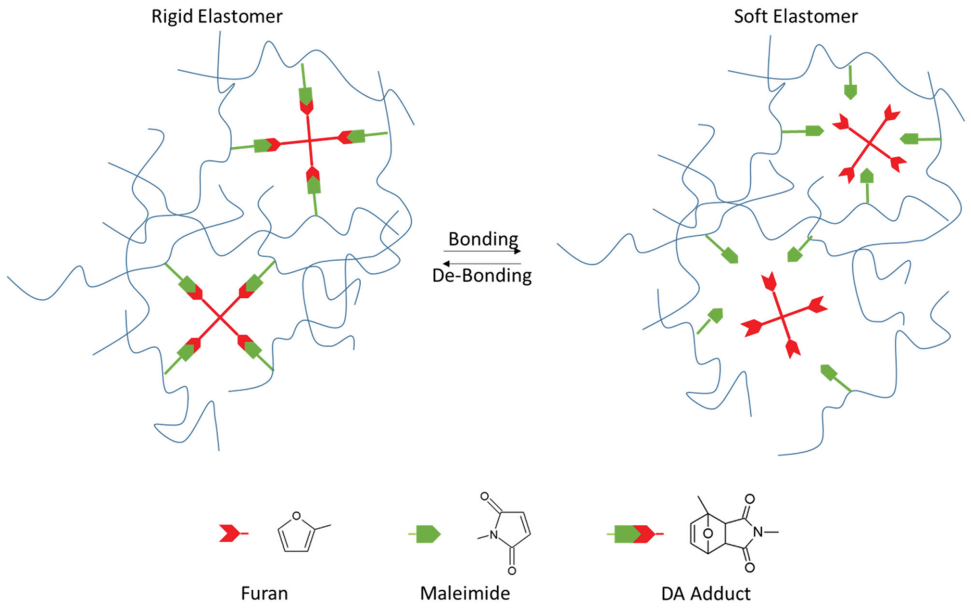

Figure 1. A schematic illustration of how the crosslinking sites are formed and broken. In this work, furan-maleimide adducts, one of the Diels–Alder pairs, were selected as the dynamic bonds forming the crosslinking sites.

maleimide derivatives as the dienophile have drawn great attention since they usually have moderate reaction (forming DA bonds) and retro-reaction (breaking DA bonds) temperatures.[15] In this work, a series of polyacrylate dielectric elastomers containing furan-maleimide adduct moieties was synthesized to exploit this reversible reaction. The resulting copolymers are elastomers exhibiting multiple states of modulus inter-switchable via thermal treatments. The rigid states have a modulus three times as high as that of the soft states. To the best of our knowledge, this is the first work tuning stiffness of elastomers using DA dynamic bonding. The elastomers were employed to fabricate capacitive sensors and actuators that could be operated in different modes.

2. Results and Discussion

2.1. Preparation of PADA Elastomer Films

2.1.1. Synthesis of Active Co-Monomer, FM-A

The active co-monomer FM-A, containing furan-maleimide DA adduct and acrylate functional groups, was synthesized following a method documented in previous work[16,17] with modifications as shown in **Figure 2**. The chemical structure of FM-A was confirmed by both ^{1}H NMR and ^{13}C NMR spectra (See Figures S1a,b, Supporting Information). Note that this furan-maleimide group on this monomer was not to provide a crosslinking site in the as-synthesized polymer but to protect the maleimide group from copolymerizing with other acrylate co-monomers.

2.1.2. Preparation of PADA Elastomer Film

Five formulations with different concentrations of co-monomers and crosslinker were investigated as shown in **Table 1**. Copolymers consisting of n-butyl acrylate (nBA) have demonstrated high actuation strains and high energy densities as dielectric elastomers.[18] Therefore, n-butyl acrylate was selected as the base monomer. 2(2-Ethoxyethoxy) ethyl acrylate (EOEA) was added to improve the solubility of FM-A in nBA. The crosslinker with four furan end groups in each molecule was previously synthesized by the same group and used in a self-healing polymer composite.[19] The copolymers are called PADA-X where X stands for the weight part of FM-A. A control formulation, PADA-10′ without crosslinker, was also synthesized. Each co-monomer, crosslinker, and a photoinitiator, 2,2-dimethoxy-2 phenylacetophenone (DMPA), were admixed at the weight ratios shown in Table 1 to afford clear solutions. Note that in all the formulations, the furan moieties and the maleimide moieties were equimolar.

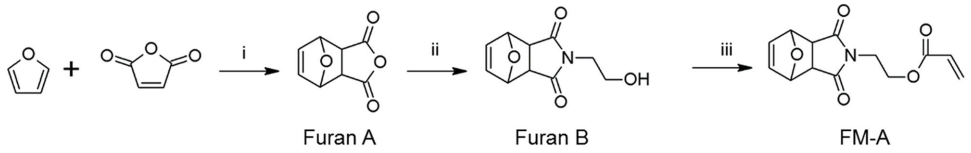

Figure 2. The synthesis route of FM-A: i) ethyl acetate, room temperature, 24 h; ii) ethanolamine, ethanol, reflux, 4 h; iii) acryloyl chloride, triethyl amine, DCM, 0 °C to room temperature, 24 h.

Table 1. Formulations (parts of weight) of synthesized elastomers.

Formulation	nBA	EOEA	FM-A	Crosslinker	DMPA
PADA-2.5	87	11	2.5	1.9	1
PADA-3	86	11	3	2.3	1
PADA-4	85	11	4	3	1
PADA-5	84	11	5	3.8	1
PADA-10	80	10	10	7.5	1
PADA-10′	80	10	10	0	1

The synthetic route for the elastomers is schematically illustrated in **Figure 3**. Elastomer films were prepared by injecting the corresponding formulation solutions into two glass slides to form a uniform liquid layer whose thickness was defined by a spacer. The liquid layer subsequently formed a solid film through ultraviolet (UV) polymerization. The three acrylate monomers (nBA, EOEA, and FM-A) copolymerized into a linear chain (Polymer 1 in Figure 3) with pendant DA adducts provided by FM-A. The crosslinker dissolved in Polymer 1 but remained intact during the UV copolymerization. The film was then heated at 130 °C for 2 h and then at 70 °C for 24 h to affect a metathetic reaction between the pendant DA moieties and the crosslinker compound: the DA moieties underwent retro-DA reaction and released furan molecules, and the resulting pendant maleimide moieties (in Polymer 2) underwent DA reaction with the furan groups on the dissolved crosslinker at 70 °C to afford a crosslinked elastomer network. The chemical structures of the two intermediate products, Polymer 1 and Polymer 2 were characterized through UV absorption spectroscopy, shown in Figure S2 (Supporting Information). The peak at 280 nm in Polymer 2's UV absorption curve corresponded to the pendent maleimide moieties, which was absent in Polymer 1. This metathetic route was taken because the maleimide moieties could participate in the free-radical co-polymerization of the acrylate groups.[20] The DA adduct with furan molecules protected maleimide moieties through the UV curing process and could be easily de-protected by retro-DA reaction. The resulted elastomer films were transparent with slight tint. The films were relatively rigid as the DA bonds were formed, and called PADA-X-r, where r indicates being rigid.

The scenario was confirmed with thermogravimetric analysis (TGA). As calculated from the formulation of PADA-10, the weight percentage of evaporated furan molecules is 2.4% theoretically. As shown in Figure S3 (Supporting Information), the as-synthesized PADA-10 sample (PADA-10-r) remained stable up to 180 °C while heating in air atmosphere at the rate of 5 °C min^{-1}. In comparison, another sample, PADA-10_70, was synthesized from the same pre-polymer solution but the heating step at 130 °C for 2 h had been skipped. Different from PADA-10-r, PADA-10_70 showed a weight loss of 2.7 wt% from 50 °C to 180 °C. As indicated in its derivative curve in Figure S3 (Supporting Information), the major weight loss of PADA-10_70 happened from 110 °C to 155 °C, which

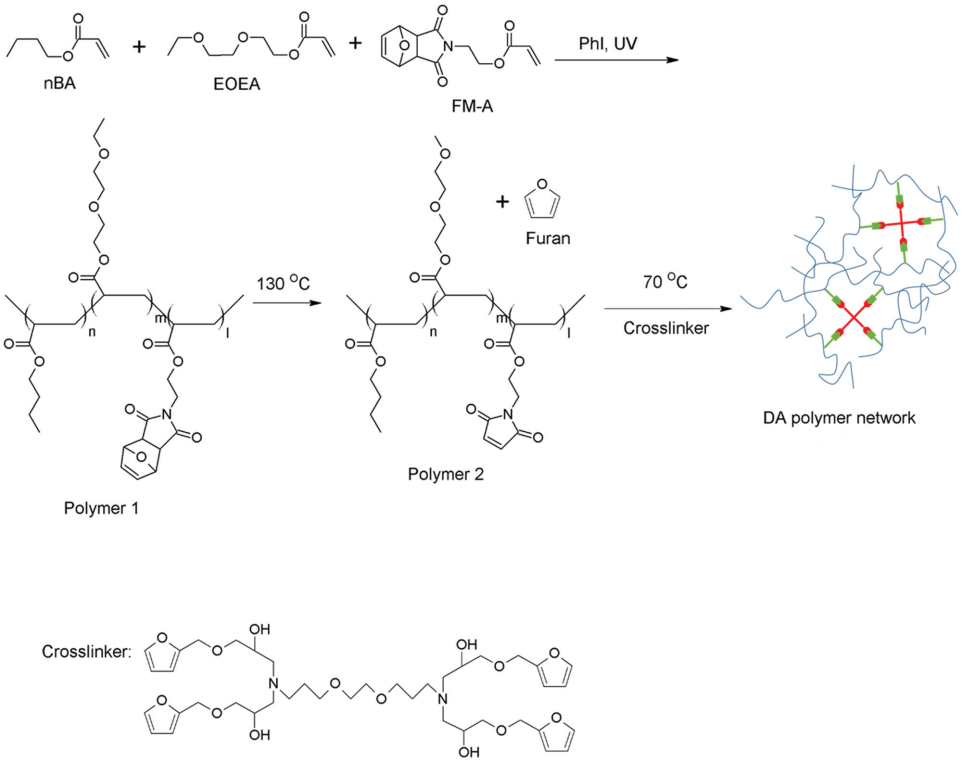

Figure 3. The synthesis route of a PADA elastomer. The co-monomers, crosslinker, and photoinitiator are admixed and subjected to UV exposure to copolymerize the three vinyl monomers. Thermal treatment at 130 °C eliminates the protecting furan group. The resulting polymer 2 is then reacting with the crosslinker at 70 °C to afford the crosslinked polymer network.

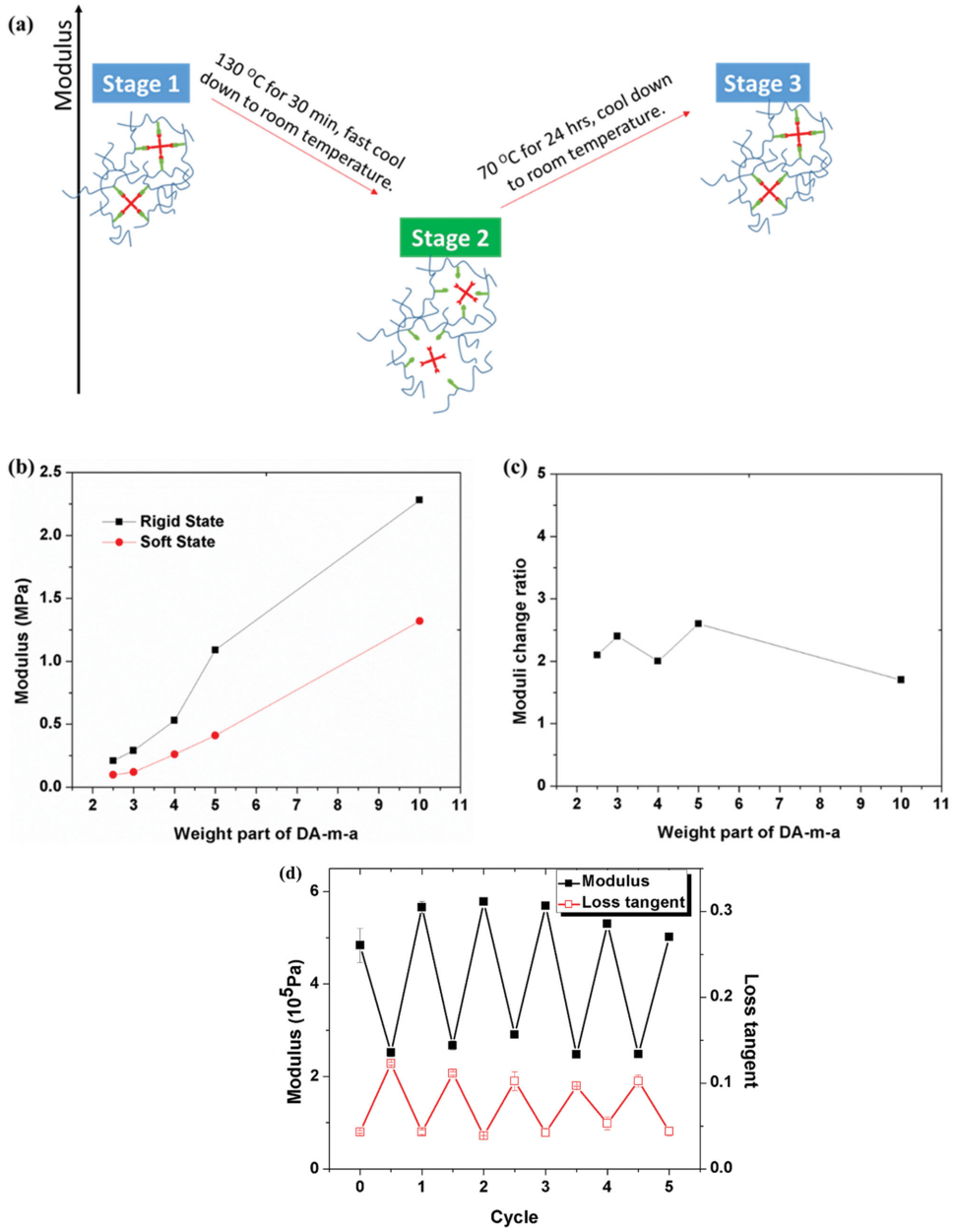

Figure 4. a) A schematic illustration of thermal treatments. The as-synthesized films were at their rigid states (Stage 1, PADA-X-r). Soft states (Stage 2, PADA-X-s) were achieved through heating the films at 130 °C for 30 min and then fast cooling down to room temperature. Rigid states (Stage 3, PADA-X-r) could be regained through heating the films at 70 °C for another 24 h and cooling down to room temperature. b) The moduli of elastomer formulations with different weight parts of FM-A at both rigid and soft states, and c) the moduli change ratio (*R*) between two states. d) Cycling test of one of the formulations, PADA-4. These elastomer samples were thermally adjusted between PADA-4-r and PADA-4-s as shown in (a) for five cycles.

had a peak value at 138 °C. The temperature range matched well with where the retro-DA reaction happened in furan-maleimide adducts and the value of weight loss was in good agreement with the theoretical calculation.[21]

2.2. Stiffness Change via Reversible DA Reaction

Since the mechanical properties of elastomers heavily depend on their crosslinking densities, forming and breaking the DA crosslinking sites would create two or more stiffness states in one elastomer. The rigid state corresponds to the highly crosslinked state as synthesized with short chain segments while the soft state is achieved by partially breaking DA bonds, resulting in long-chain segments between crosslinking sites. The soft elastomer could return to its rigid state by reforming DA bonds. As shown in **Figure 4**a, Stage 1 samples refer to those as-synthesized (PADA-X-r). The Stage 2 (PADA-X-s) samples were obtained by heating PADA-X-r samples at 130 °C for 30 min followed by fast cooling down to room temperature.

Table 2. Moduli of the formulated elastomers at three stages in one cycle.

Elastomer	Stage 1 (PADA-X-r)		Stage 2 (PADA-X-s)		Stage 3 (PADA-X-r)	
	E' [MPa]	tan δ	E' [MPa]	tan δ	E' [MPa]	tan δ
PADA-2.5	0.20 ± 0.02	0.118 ± 0.008	0.099 ± 0.003	0.271 ± 0.006	0.214 ± 0.003	0.114 ± 0.003
PADA-3	0.30 ± 0.02	0.08 ± 0.01	0.12 ± 0.01	0.22 ± 0.03	0.27 ± 0.02	0.09 ± 0.01
PADA-4	0.52 ± 0.03	0.045 ± 0.008	0.26 ± 0.02	0.10 ± 0.02	0.54 ± 0.03	0.039 ± 0.003
PADA-5	1.23 ± 0.09	0.026 ± 0.004	0.41 ± 0.03	0.084 ± 0.009	0.94 ± 0.06	0.033 ± 0.003
PADA-10	2.24 ± 0.09	0.026 ± 0.001	1.32 ± 0.06	0.031 ± 0.001	2.31 ± 0.07	0.026 ± 0.001
PADA-10′	1.01	0.028	1.06	0.026	–	–

The Stage 3 samples (also PADA-X-r) were obtained by heating the PADA-X-s samples at 70 °C for 24 h. All elastomer samples were tested at least for one cycle in three stages and five samples were tested for each formulation except PADA-10′. The elastic moduli (E') and loss tangents (tan δ) were measured using a dynamic mechanical analyzer (DMA) and listed in **Table 2**. All the formulations showed an obvious difference in modulus between Stage 1/3 and Stage 2 except PADA-10′. This proved that it was the dynamic DA bonding/debonding that contributed to the change of moduli.

As demonstrated in Table 2 and **Figure 5**b, at both rigid and soft state, the moduli of the formulated elastomers increased with the addition of FM-A and crosslinker. The increase of moduli can be attributed to the increase of crosslinking density. Another reason is the addition of rigid monomer. Compared with nBA and EOEA, FM-A has a relatively bulky and rigid side group, which hardens of the elastomers. The moduli change ratio (R), between rigid and soft states, of an elastomer is calculated from the data in the first cycle using the equation:

$$R = \frac{E'_{\text{Stage1}} + E'_{\text{Stage3}}}{2 \times E'_{\text{Stage2}}} \quad (3)$$

All the elastomers displayed very similar moduli change ratio, around 2, which indicated that the chain segment length was doubled in the soft state and half of the crosslinking sites were broken.

The elastomers could be adjusted from PADA-X-r and PADA-X-s repeatedly thanks to the good reversibility of the DA reactions. One of the elastomers, PADA-4, was tested for five cycles as shown in Figure 4d. Both moduli and loss tangents were consistently modulated between rigid and soft states.

2.3. Achieving Variable Stiffness by Controlling Crosslinking Density

Multiple states of stiffness could also be achieved through treatments at different temperatures as the equilibrium state of the reversible bonding (DA) and de-bonding (retro-DA) reactions could be shifted by temperature change. Higher de-bonding temperatures (>90 °C) leads to more de-bonding and thus lower stiffness, while lower temperature (≈70 °C) result in higher crosslinking density and stiffness.[22] For instance, PADA-4-r elastomers were heated at different de-bonding temperatures, 90 °C, 110 °C, 130 °C, or 160 °C, and then rapidly cooled down to room temperature (step i in Figure 5), and the resulting elastomers were designated

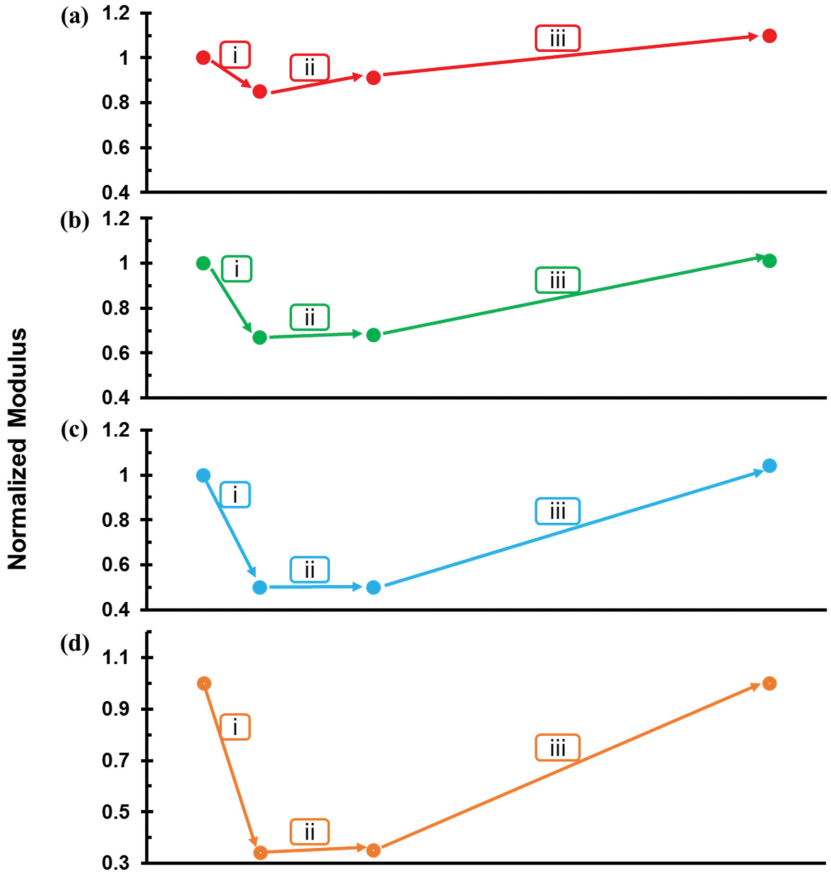

Figure 5. Various moduli could be achieved for PADA-4 elastomers via thermal treatments. i) PADA-4-r samples were heated at a) 90 °C, b) 110 °C, c) 130 °C, and d) 160 °C followed by a fast cooling down to room temperature to obtain PADA-4-s90, PADA-4-s110, PADA-4-s, and PADA-4-s160. ii) Samples were aged at room temperature for 2 h. iii) Samples were heated at 70 °C for 24 h in (a), (b), and (c) and for 48 h in (d). Moduli were normalized as the modulus of PADA-4-r was set as 1.

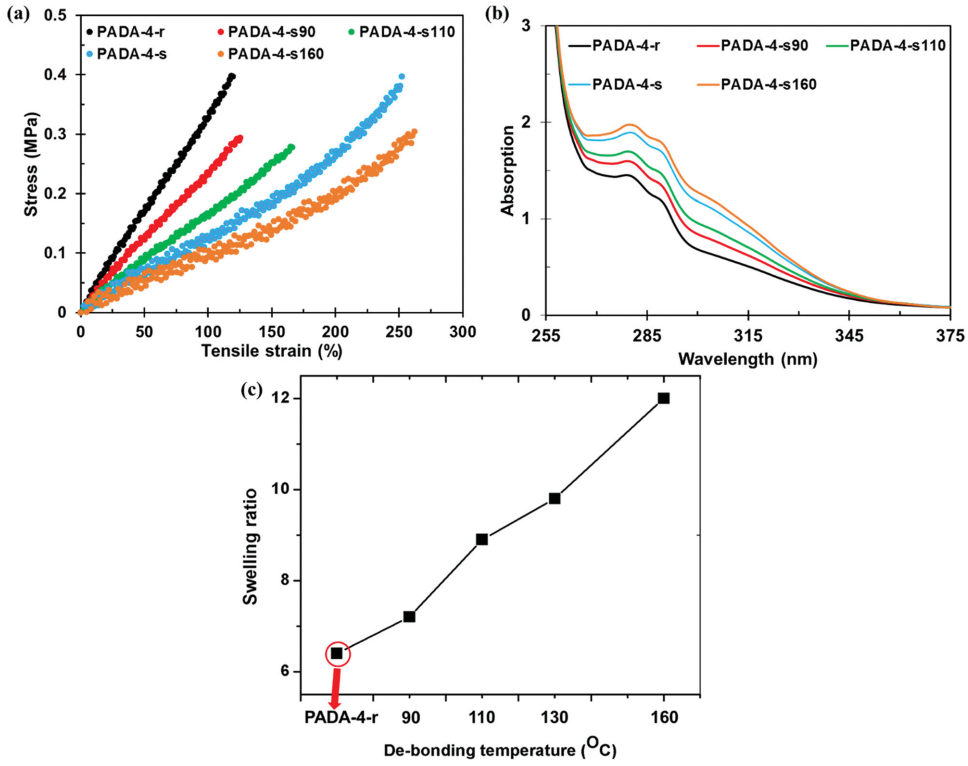

Figure 6. a) Stress–strain curves of PADA-4 elastomers measured using dumbbell-shaped samples stretched to rupture at 3.33 mm s^{-1}. b) UV absorption spectra of PADA-4 thin films with a thickness of 100 μm. c) Swelling ratios of PADA-4 elastomers in chloroform.

as PADA-4-s90, PADA-4-s110, PADA-4-s, and PADA-4-s160, respectively. While PADA-4-s had a modulus equal to half of that of PADA-4-r, the ratios of the moduli of PADA-4-s90, PADA-4-s110, and PADA-4-s160 to that of PADA-4-r were 0.85, 0.67, and 0.34 measured with DMA, respectively. After aging at room temperature for 2 h (step ii in Figure 5), the moduli of PADA-4-s90, PADA-4-s110, PADA-4-s, and PADA-4-s160 did not show a significant increase. Generally, DA reaction is thermodynamically favorable to the retro-DA at room temperature. Therefore, PADA-4-r should be the thermodynamically stable form of all the PADA-4 series of elastomers at room temperature. However, the soft states could be maintained for a relatively long time due to the slow DA reaction, which is required for many applications. After heating at 70 °C for 24 h (step iii in Figure 5a–c), PADA-4-s90, PADA-4-s110, and PADA-4-s regained their original stiffness. However, PADA-4-s160 needed 48 h heating at 70 °C (step iii in Figure 5d) to return to the original modulus.

The PADA-4 series of elastomers were further characterized through tensile testing, UV spectroscopy, and swelling testing, to correlate the change of modulus to molecular crosslinking density. The stress–strain responses of the elastomers are displayed in **Figure 6**a. Higher de-bonding temperature resulted in a softer elastomer with larger elongation at rupture, which can be attributed to the decrease of crosslinking density.[23] Note that PADA-4-s has a lower modulus than those of PADA-4-r, but its strength at rupture is comparable to that of PADA-4-r, indicating a greater toughness. This superior mechanical property could be explained using elastomer's bimodal theory that in a crosslinking network, long chains contribute to the elastomer's extensibility while short chains correspond to high stress.[24] Based on the toughness shown in Figure 6a, among the PADA-4 series, PADA-4-s might have the most optimal chain length distribution.

UV absorption spectra (Figure 6b) allows direct measurement of the extent of DA/retro-DA reaction. The peak at 280 nm corresponds conjugated O=C–C=C–C=O structure in maleimide moieties, and its intensity increases with elevated de-bonding temperatures. The portions (x) of furan and maleimide pairs that had formed DA adduct were calculated based on the peak intensity at 280 nm following the method in Imai et al.,[25] and the average molecular weight of chain segments between crosslinkes, $\overline{M_C}$, of each elastomer was related to x using Equation (4)

$$\overline{M_C} = \frac{\overline{M_{C0}}}{x} \tag{4}$$

where $\overline{M_{C0}}$ is the average molecular weight of chain segments between crosslinks in PADA-4-r.

The crosslinking density was alternatively estimated by swelling. The elastomer films were cut into round plates and swelled in chloroform for 16 h. The swelling ratio Q is defined as

$$Q = \left(\frac{a}{a_0}\right)^3 \tag{5}$$

where a and a_0 are the diameter of the plates after and before swelling, respectively. $\overline{M_C}$ can be calculated using

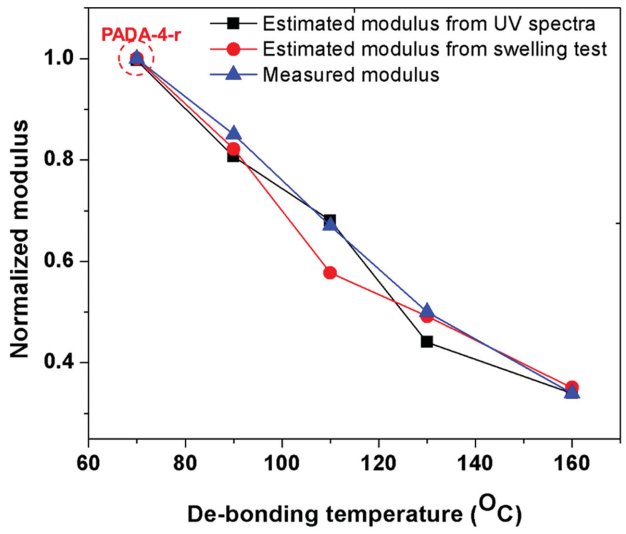

Figure 7. Estimated moduli from both UV absorption spectra and swelling test and DMA measured moduli of samples at different de-bonding temperature. Moduli were normalized as the modulus of PADA-4-r was set as 1.

$$\overline{M_C} = \frac{2\rho V_1 Q^{\frac{5}{3}}}{(1-K)} = \overline{M_{C0}}\left(\frac{Q}{Q_0}\right)^{\frac{5}{3}} \quad (6)$$

where V_1, Q_0, and K are the molar volume of the solvent (chloroform in this case), swelling ratio of PADA-4-r in chloroform and a constant related to temperature, polymer, solvent, and their interaction, respectively.[26]

Moduli of PADA-4 elastomers were estimated using Equation (2) from $\overline{M_C}$ values obtained from both UV absorption spectra and swelling test. The estimated values and measured values from DMA were displayed in **Figure 7** for comparison. The measured moduli matched well with the calculated moduli, indicating that it is the crosslinking density of the elastomer that alters the stiffness of the PADA-4 elastomers.

2.4. Applications

Good dielectric elastomers should be soft so that they are sensible to small pressure changes, can detect large deformations, and exert large actuation strain. On the other hand, soft elastomers with low modulus could suffer from low structural support and electromechanical instability.[26] PADA-4 was selected to fabricate sensors and actuators thanks to its moderate moduli in both rigid and soft states. Among PADA-4 elastomers, PADA-r and PADA-s were compared.

2.4.1. Capacitive Sensing

These capacitors, whose structure is illustrated in **Figure 8**a, had a width of 6 cm and an active length of 2 cm. The area with electrodes overlapping was 5 cm × 2 cm to avoid shorting near contacts. As indicated by the stress–strain curves of the sensors made of PADA-4-r and PADA-4-s in Figure 8b, these sensors could be operated in two modes with different mechanical loadings.

The sensing performance was tested with a linear stage to stretch the film at 1 mm s^{-1} and a self-sensing unit to measure the capacitance at 400 Hz. Note that in Figure 8cd, the thickness (d) of the capacitor is normalized to 100 µm (d_0). The capacitances had a quasi-linear relationship with the stretch strain up to 30% linear strain, which is good for strain sensing purpose. As converted from Figure 8b,c, mechanical pressures also displayed a quasi-linear relationship with the capacitances. This sensor can potentially be integrated into more complex devices with multiple working modes: a high sensitivity mode with low mechanical pressure load and a high mechanical pressure mode with lower sensitivity. Two examples are knee pads with standby mode and active mode and flexible electronics with press mode and stretch mode.[27]

As calculated from the measured capacitances at 0% strain, the dielectric constants (ε_r) of PADA-4-r and PADA-4-s are 5.7 and 6.3, respectively. The reason the dielectric constant of the PADA-4-s is slightly higher than that of PADA-4-r could be due to less confinement of dipoles in the softer polymer network.[28]

2.4.2. Actuation

Actuators were fabricated with 5% by 5% biaxial prestrain to avoid wrinkling during actuation.[29] Carbon grease was coated on both sides of the stretched films as electrodes. Voltages were applied at each nominal 10 MV m^{-1} increments. The change of the actuator's active areas, defined as the overlapping area of two electrodes, was recorded by a web camera controlled by a LabView program. For both rigid and soft DA-4 films, four samples were tested and the average data are presented in **Figure 9**.

As indicated in Equation (1), the actuation strain is dependent on the elastomer's dielectric constant, mechanical modulus, and the actuation electric field. Different from most elastomers which would show a certain actuation strain at a particular electric field, this elastomer was able to produce different actuation performances at identical electric fields. This is particularly important when constant actuation pressure and various actuation strains are needed at the same time.

Key actuation performances of the two states are listed in **Table 3**. The dielectric strength is calculated as the real electric field at the breakdown point. Average value of four actuators in each group is presented. The actuation pressure (P) and energy density ($\frac{1}{2}e$) were calculated using Equations (7) and (8):[30]

$$P = \varepsilon_0 \varepsilon_r E^2 \quad (7)$$

$$\frac{1}{2}e = -\frac{1}{2}\varepsilon_0 \varepsilon_r E^2 \ln(1+s_z) \quad (8)$$

PADA-4 films had comparable energy densities with other dielectric elastomers with low prestrain ratios.[31] PADA-4-r had

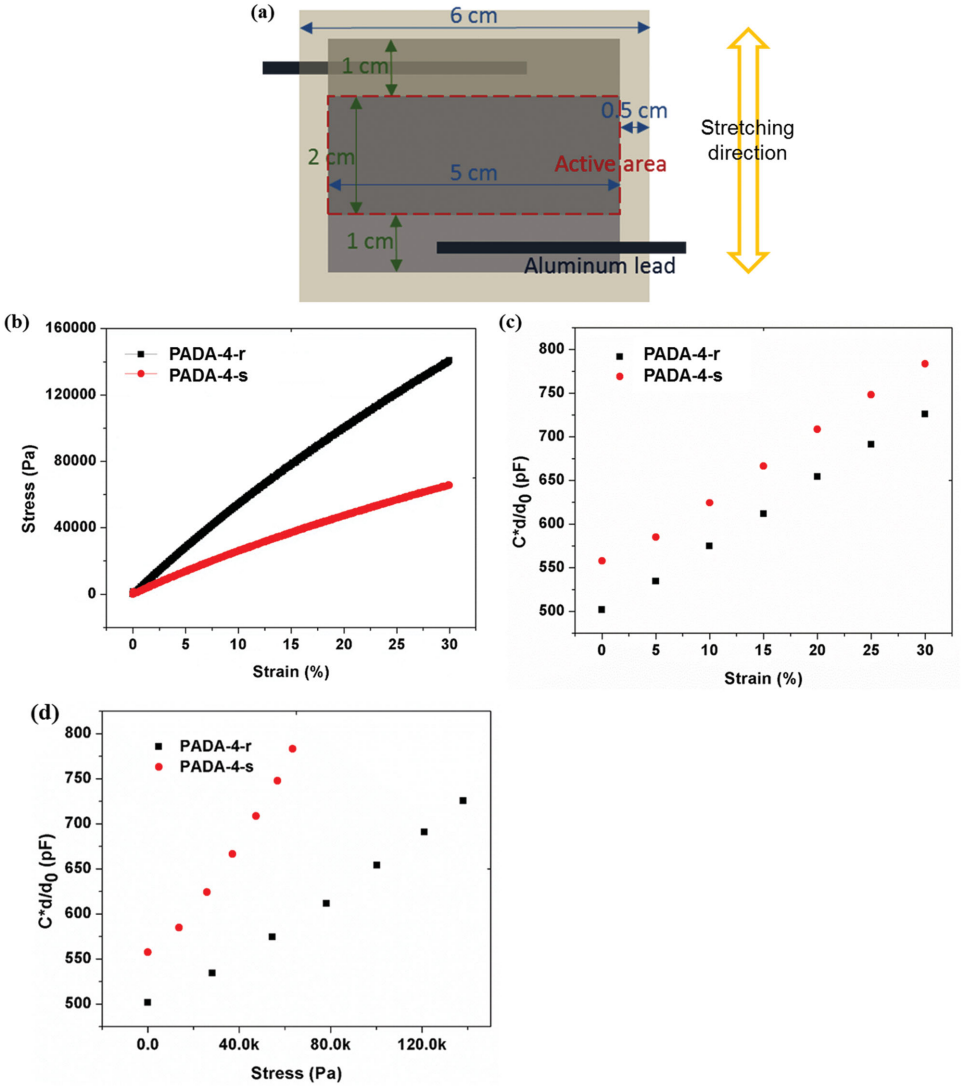

Figure 8. a) The structure of a capacitive sensor. b) The stress–strain curves of the sensors made of PADA-4-r and PADA-4-s at a stretch rate of 1 mm s^{-1}. c) The capacitive sensing results at a stretch rate of 1 mm s^{-1}. d) The capacitance–stress curves of the sensors. Note that in (c,d), the thickness of the capacitor is normalized to 100 (d_0).

an overall better performance than PADA-4-s did since it had a higher dielectric strength. This could be attributed to a higher modulus of the rigid film, which can help prevent electromechanical instability.[32] Additionally, some mobile crosslinker molecules inside the PADA-4-s network might result in a leakage current increase, which would assist dielectric breakdown.[26] Therefore, PADA-4-r is more suitable to be used in applications needing higher force output and energy density. However, at certain electric fields, PADA-4-s had a larger strain than PADA-4-r had, which made it useful for applications requiring higher strain at reduced operation voltages.

3. Conclusion

In this work, a new group of dielectric elastomers with furan-maleimide dynamic covalent bonding were synthesized and characterized. The moduli of these elastomers can be tuned reversibly and incrementally by controlling the crosslinking densities of the polymer networks through the Diels–Alder reversible reactions. The moduli change ratio was limited by the incomplete retro-Diels-Alder reaction. The elastomers' moduli at their rigid states were three times of those at the corresponding soft states.

The synthesized elastomers were further fabricated into capacitive sensors, which could work in both high/low mechanical loading modes and actuators, which could work in high strain or high force output modes. These devices could be integrated into more complex electromechanical systems with variable work conditions. Going forward, the proposed dielelectric elastomer would be used in energy generators to match various mechanical inputs.

4. Experimental Section

Preparation of PADA Elastomer Films: The active co-monomer, FM-A was synthesized as described in Section S1 (Supporting Information).

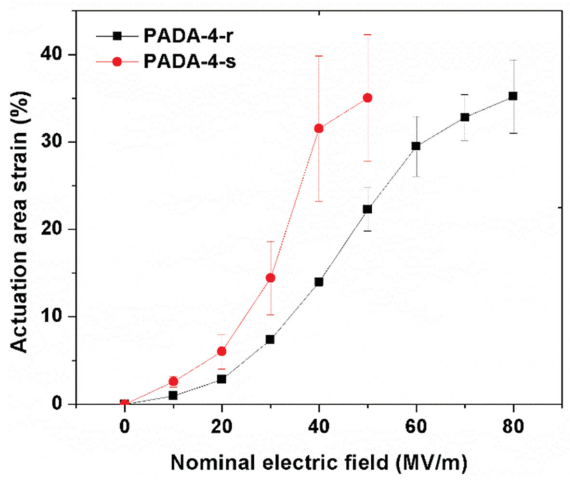

Figure 9. Actuation curves of PADA-4-r and PADA-4-s. Average actuation strains at each nominal 10 MV m^{-1} electric field were plotted. Both films were prestretched 5% by 5%.

N-butyl acrylate and 2,2-dimethoxy-2 phenylacetophenone were purchased from Sigma–Aldrich and used as received. 2(2-Ethoxyethyoxy) ethyl acrylate was obtained from Sartomer Company and used as received. The crosslinker was synthesized following the method in Gong et al. [19] published by the same group. To prepare a PADA elastomer film, a pre-polymer solution was made by co-dissolving all the components as listed in Table 1. The solution was injected into two glass slides coated with commercial Rain-X Original Glass Water Repellent with a spacer to define the thickness of the liquid layer. The liquid layer was first cured through a conveyer equipped with a 2.5 W cm^{-2} Fusion 300S type H UV curing bulb, at a speed of 4.0 feet min^{-1} for two passes. The resulted film was gently removed off the glass slides and then heated at 130 °C for 2 h followed by another 24-h heating at 70 °C, effecting a metathetic reaction to form the crosslinked network. The as synthesized films were named as PADA-X-r. To understand the metathetic procedure, a control sample film, PADA-10_70 was synthesized from PADA-10 solution and through the same method but the step, heating at 130 °C, was skipped. Both PADA-10_70 and PADA-10-r were characterized using a PerkinElmer Pyris Diamond TGA with a heating rate of 5 °C min^{-1} in air atmosphere from 50 °C to 180 °C.

Stiffness Change via Reversible DA Reaction: The moduli and loss tangents of PADA elastomer films at various stages were measured with a TA RSA3 DMA. A rectangular shaped film sample with a thickness of ≈100 µm, a width of ≈5 mm was loaded onto the DMA with an active length of ≈10 mm. Typically, a tension strain (<3%) was applied at 1 Hz frequency. In one stiffness change cycle, Stage 1 in Figure 4 a and Table 2 referred to the as synthesized (PADA-X-r), Stage 2 samples (PADA-X-s) were achieved via heating the PADA-X-r samples at 130 °C for 30 min followed by fast cooling down to room temperature via compressed air blowing. Thereafter, PADA-X-s elastomers were heated at 70 °C for 24 h and cooled down to room temperature to obtain PADA-X-r (Stage 3) again. All PADA elastomers were tested at least for one cycle except the control sample PADA-10, ′ whose moduli were measured only at Stages 1 and 2. To determine the reversibility, one of the PADA elastomers, PADA-4, was tested for five cycles.

Table 3. Comparison of the actuation performances of PADA-4-r and PADA-4-s.

Property	Max are strain [%]	Dielectric strength [MV m^{-1}]	Max actuation pressure [MPa]	Max energy density [kJ m^{-3}]
PADA-4-r	35 ± 4	104 ± 10	0.55	83
PADA-4-s	35 ± 7	65 ± 7	0.24	36

Achieving Variable Stiffness by Controlling Crosslinking Density: To achieve multiple states of stiffness, one of the PADA elastomers, PADA-4-r was heated at 90 °C, 110 °C, 130 °C, and 160 °C and then fast cooled down to room temperature through compressed air blowing. Resulted elastomers were named as PADA-4-s90, PADA-4-s110, PADA-4-s, and PADA-4-s160, respectively. Moduli of these PADA-4 samples were measured though DMA as described before. These samples were aged at room temperature for 2 h and their moduli were recorded. Then these elastomers were heated at 70 °C for 24 h or 48 h and cooled down to room temperature followed by the measurement of their moduli. The tensile stress–strain behaviors of PADA-4 elastomers were tested on the same DMA. A sample had a standard dumbbell shape with an active length of 12 mm and a width of 2 mm and stretched at 3.33 mm s^{-1} till rupture. The UV absorption spectra PADA-4 films were obtained using a Shimadzu ParmaSpec UV-1700 UV-Visible spectrophotometer. These films with thickness of ≈100 µm were prepared using quartz slides as the mold instead of regular glass slides. After curing, one of the quartz slides was carefully peeled off resulting in the film attaching on the other quartz during further thermal treatment and measurement. PADA-4 elastomers were further characterized in swelling test. In a typical procedure, a film was cut into round-shaped plates and swelled in chloroform for 16 h. The diameters of the plate before and after swelling were measured.

Application as Capacitive Sensor: PADA-4-r and PADA-4-s were fabricated into capacitive sensors. CNT was sprayed onto the both sides of a film as the electrodes. The area of one sensor was 6 cm × 2 cm within which an area of 2 cm × 5 cm had overlapped electrodes (the area of the capacitor). The stress–strain curves of the capacitive sensors were tested on a TA RSA3 DMA at a stretch rate of 1 mm s^{-1}. The capacitors were further stretched using a Zaber A-LSQ300A-E-1 motorized linear stage at the same rate. Meanwhile the capacitances were measured on a SSU developed in the Biomimetics Laboratory in the University of Auckland, New Zealand. During measurement, a sinusoidal AC signal with an amplitude of 50 V and an average of 400 V at 400 Hz was applied.

Application as Actuator: PADA-4-r and PADA-4-s were fabricated into actuators with 5% by 5% biaxial prestrain. One actuator had a round shape with a ¼ inch diameter. Carbon grease was coated onto both sides of the films as electrodes. High voltages were supplied from the HV box fabricated in-house. The area change of the active area, defined as the overlapping area of the two electrodes, was recorded by a web camera controlled by a LabView program. Voltages were applied to obtain 10 MV m^{-1} increments in the nominal electric field regarding to the unactuated thickness of each film. Four samples were tested for both rigid and soft films, respectively.

Supporting Information

Supporting Information is available from the Wiley Online Library or from the author.

Acknowledgements

The work reported here was financially supported by the US National Science Foundation, Award # 1207975.

Received: April 16, 2015
Revised: May 21, 2015
Published online: July 1, 2015

[1] A. O'Halloran, F. O'Malley, P. McHugh, *J. Appl. Phys.* **2008**, *104*, 071101.
[2] P. Brochu, Q. Pei, *Macromol. Rapid Commun.* **2010**, *31*, 10.

[3] C. Keplinger, T. Li, R. Baumgartner, Z. Suo, S. Bauer, *Soft Matter* **2012**, *8*, 285.
[4] H. Böse, E. Fuß, *Proc. SPIE* **2014**, *9056*, 905614.
[5] P. Maiolino, F. Galantini, F. Mastrogiovanni, G. Gallone, G. Cannata, F. Carpi, *Sens. Actuators A. Phys.* **2015**, *226*, 37.
[6] R. Pelrine, R. Kornbluh, J. Joseph, R. Heydt, Q. Pei, S. Chiba, *Mater. Sci. Eng. C* **2000**, *11*, 89.
[7] C. Murray, D. McCoul, E. Sollier, T. Ruggiero, X. Niu, Q. Pei, D. Di Carlo, *Microfluid. Nanofluid.* **2013**, *14*, 345.
[8] O. A. Araromi, I. Gavrilovich, J. Shintake, S. Rosset, M. Richard, V. Gass, H. R. Shea, *IEEE/ASME Trans. Mechatronics* **2015**, *20*, 438.
[9] K. Shanmuganathan, J. R. Capadona, S. J. Rowan, C. Weder, *Prog. Polym. Sci.* **2010**, *35*, 212.
[10] J. M. Ginder, S. M. Clark, W. F. Schlotter, M. E. Nichols, *Int. J. Mod. Phys. B* **2002**, *16*, 2412.
[11] E. Verploegen, J. Soulages, M. Kozberg, T. Zhang, G. McKinley, P. Hammond, *Angew. Chem. Int. Ed.* **2009**, *48*, 3494.
[12] X. Niu, X. Yang, P. Brochu, H. Stoyanov, S. Yun, Z. Yu, Q. Pei, *Adv. Mater.* **2012**, *24*, 6513.
[13] S. L. Rosen, *Fundamental Principles of Polymeric Materials,* Wiley-Interscience, New York **1993**.
[14] Y.-L. Liu, T.-W. Chuo, *Polym. Chem.* **2013**, *4*, 2194.
[15] X. Chen, M. A. Dam, K. Ono, A. Mal, H. Shen, S. R. Nutt, K. Sheran, F. Wudl, *Science* **2002**, *295*, 1698.
[16] S. Yu, R. Zhang, Q. Wu, T. Chen, P. Sun, *Adv. Mater.* **2013**, *25*, 4912.
[17] M. Liu, J. van Hensbergen, R. P. Burford, A. B. Lowe, *Polym. Chem.* **2012**, *3*, 1647.
[18] W. Hu, X. Niu, X. Yang, N. Zhang, Q. Pei, *Proc. SPIE* **2013**, *8687*, 86872U.
[19] C. Gong, J. Liang, W. Hu, X. Niu, S. Ma, H. T. Hahn, Q. Pei, *Adv. Mater.* **2013**, *25*, 4186.
[20] F. Morel, C. Decker, S. Jönsson, S. C. Clark, C. E. Hoyle, *Polymer* **1999**, *40*, 2447.
[21] A. Gandini, *Prog. Polym. Sci.* **2013**, *38*, 1.
[22] Y.-L. Liu, C.-Y. Hsieh, Y.-W. Chen, *Polymer* **2006**, *47*, 2581.
[23] L. González, A. Rodríguez, J. L. Valentin, A. Marcos-Fernández, P. Posadas, *Elastom. Kunststofee* **2005**, *58*, 638.
[24] J. E. Mark, *Acc. Chem. Res.* **1994**, *27*, 271.
[25] Y. Imai, H. Itoh, K. Naka, Y. Chujo, *Macromolecules* **2000**, *33*, 4343.
[26] X. Niu, H. Stoyanov, W. Hu, R. Leo, P. Brochu, Q. Pei, *J. Polym. Sci., Part B: Polym. Phys.* **2013**, *51*, 197.
[27] D. J. Lipomi, M. Vosgueritchian, B. C.-K. Tee, S. L. Hellstrom, J. a. Lee, C. H. Fox, Z. Bao, *Nat. Nanotechnol.* **2011**, *6*, 788.
[28] Q. M. Zhang, J. Su, C. H. Kim, R. Ting, R. Capps, *J. Appl. Phys.* **1997**, *81*, 2770.
[29] G. Kofod, P. Sommer-Larsen, R. Kornbluh, R. Pelrine, *J. Intell. Mater. Syst. Struct.* **2003**, *14*, 787.
[30] R. Pelrine, R. Kornbuh, Q. Pei, J. Joseph, *Science* **2000**, *287*, 836.
[31] P. H. Vargantwar, A. E. Özçam, T. K. Ghosh, R. J. Spontak, *Adv. Funct. Mater.* **2012**, *22*, 2100.
[32] X. Zhao, Z. Suo, X. Zhao, Z. Suo, *Phys. Rev. Lett.* **2010**, *104*, 178302.